THE JOURNAL OF PHYSICAL CHEMISTRY A

Article

pubs.acs.org/JPCA

Local Electronic Structure in γ-$LiAlO_2$ Studied by Single-Crystal ^{27}Al NMR and DFT Calculations

Thomas Bräuniger,*[,†] Burkhard Groh,[†] Igor L. Moudrakovski,[‡] and Sylvio Indris*[,§]

[†]Department of Chemistry, University of Munich (LMU) Butenandtstr. 5−13, 81377 Munich, Germany

[‡]Max-Planck-Institute for Solid-State Research, Heisenbergstr. 1, 70569 Stuttgart, Germany

[§]Karlsruhe Institute of Technology, Institute for Applied Materials (IAM), Hermann-von-Helmholtz-Platz 1, 76344 Eggenstein-Leopoldshafen, Germany

ABSTRACT: From single-crystal ^{27}Al NMR experiments, the full tensors for both the electrical field gradient (EFG) and the chemical shift (CS) for the aluminum atoms in γ-$LiAlO_2$ have been determined. A simultaneous fit of the quadrupolar splittings observed for the four ^{27}Al in the unit cell gave the EFG tensor in the crystal frame, from which a quadrupolar coupling constant of $\chi = C_Q = 3.330 \pm 0.005$ MHz and an asymmetry parameter of $\eta_Q = 0.656 \pm 0.002$ were derived. The experimentally determined quadrupolar splittings were sufficiently sensitive to quantify small deviations of both rotation axis direction and starting direction by the data fitting routine. For determination of the CS tensor, the evolution of the outer satellite centers over the crystal rotation was tracked, and the contribution of the quadrupolar shift was subtracted according to the previously determined EFG tensor. The resulting CS tensor of ^{27}Al yields an isotropic chemical shift of $\delta_{iso} = 81.8 \pm 0.25$ ppm and an asymmetry parameter of $\eta_{CS} = 0.532 \pm 0.004$, in good agreement with the fit of a MAS NMR spectrum acquired at $B_0 = 21.1$ T. From both experiments and DFT calculations using the CASTEP code, we find the eigenvectors of the EFG and CS tensors to be practically colinear.

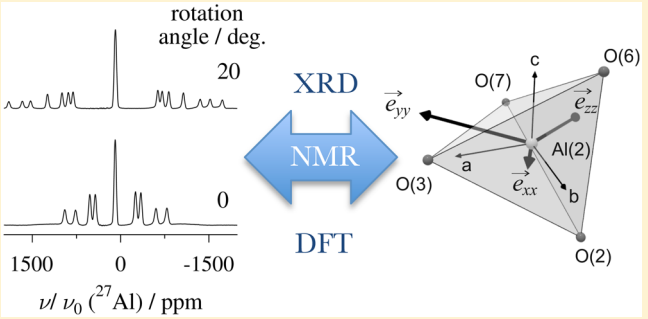

1. INTRODUCTION

The tetragonal modification of lithium aluminate, γ-$LiAlO_2$, has been studied by several analytical techniques, including nuclear magnetic resonance (NMR) spectroscopy,[1−3] X-ray,[4] and neutron diffraction.[5] The interest in $LiAlO_2$ partly stems from the fact that the compound has several technological applications, for example, as coating material for lithium electrodes[6] and as an additive in composite lithium electrolytes.[7] γ-$LiAlO_2$ crystallizes in space group $P4_12_12$ with lattice parameters $a = b = 5.1687$ Å and $c = 6.2679$ Å. The lithium as well as the aluminum atoms are located inside distorted oxygen tetrahedra, with each LiO_4 tetrahedron sharing an edge with an AlO_4 tetrahedron.[4] These LiO_4−AlO_4 pairs are connected via common oxygen corners and form a three-dimensional lattice, as may be seen from Figure 1. There are four formula units per unit cell, but only one in the asymmetric unit. The symmetry-related units are generated by 4-fold screw axes, which are oriented parallel to the crystallographic c axis and positioned at the midpoints of the a and b axes. Therefore, for both lithium and aluminum, there are four sites in the unit cell that are chemically but not magnetically equivalent (Figure 1).

Recently, the distribution of electron density in γ-$LiAlO_2$ was investigated in detail using ^7Li NMR of single crystals, supported by density functional (DFT) calculations.[1] The well-defined orientation dependence of the NMR resonance positions in single-crystal NMR allows for determination of not just the exact magnitude but also the precise orientation of the electrical field gradient (EFG) and chemical shift (CS) tensors within the crystal lattice. In the present work, we have derived the EFG and CS tensors for the aluminum atoms in γ-$LiAlO_2$ from both single-crystal and magic-angle spinning (MAS) ^{27}Al NMR experiments, again augmented by DFT calculations. Before discussing the results, the underlying principles of our main experimental technique, that is, single-crystal NMR of ^{27}Al, will be briefly reviewed.

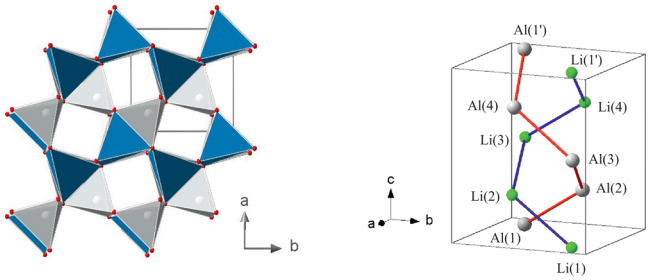

Figure 1. View of the crystal structure down the c axis (left) and location of Li and Al in the unit cell (right) of γ-$LiAlO_2$.

Received: July 20, 2016
Revised: September 15, 2016
Published: September 29, 2016

DOI: 10.1021/acs.jpca.6b07286
J. Phys. Chem. A 2016, 120, 7839−7846

2. ^{27}Al NMR OF γ-LiAlO$_2$ SINGLE CRYSTALS

Aluminum occurs only as ^{27}Al, a nucleus with spin $I = 5/2$. For the analysis of the ^{27}Al NMR spectra and their dependencies on the orientation of the single crystal, the Hamiltonian is[8−10]

$$\hat{H} = \hat{H}_Z + \hat{H}_Q + \hat{H}_{CS} \tag{1}$$

Here, $\hat{H}_Z$ is the nuclear Zeeman term and $\hat{H}_{CS}$ is the energy change caused by the chemical shift (CS) as described by the tensor $\boldsymbol{\delta}$:

$$\hat{H}_{CS} = -\gamma_n \vec{B}_0 \boldsymbol{\delta} \hat{I} \tag{2}$$

$\hat{H}_Q$ describes the nuclear quadrupole interaction and may be expressed as

$$\hat{H}_Q = \frac{eQ}{2I(2I-1)\hbar} \hat{I}\cdot\mathbf{V}\cdot\hat{I} \tag{3}$$

where $\mathbf{V}$ is the electric field gradient (EFG) tensor at the site of the nucleus, $\hat{I}$ is the nuclear spin vector, e is the elementary charge, $\hbar$ Planck's constant, and Q the nuclear quadrupole moment, which for ^{27}Al is $Q = (146.6 \pm 1.0)$ mb.[11]

The Electrical Field Gradient (EFG) Tensor. The quadrupolar interaction[8−10] is the electrical interaction between the nonsymmetric charge distribution of nuclei with spin $I > 1/2$ (gauged by eQ) and the electronic surroundings of the nucleus, gauged by the largest eigenvalue of the EFG tensor, $V_{zz}^{PAS} = eq$. The magnitude of the quadrupolar interaction is usually quantified by the quadrupolar coupling constant,

$$\chi = C_Q = \frac{eQeq}{\hbar} \tag{4}$$

and the asymmetry of the tensor by the parameter

$$\eta_Q = \frac{V_{xx}^{PAS} - V_{yy}^{PAS}}{V_{zz}^{PAS}} \tag{5}$$

where the eigenvalues of $\mathbf{V}^{PAS}$ are ordered according to the convention:

$$|V_{zz}^{PAS}| \geq |V_{yy}^{PAS}| \geq |V_{xx}^{PAS}| \tag{6}$$

If nonzero, the quadrupolar interaction lifts the degeneracy of the $2I$ NMR transitions existing under $\hat{H}_Z + \hat{H}_{CS}$. For quadrupolar nuclei with half-integer spin, it is customary to separate the transitions into two main classes according to the change of the magnetic quantum number. Thus, the $|-1/2\rangle \rightarrow |+1/2\rangle$ transition is usually termed the "central transition" (CT), and the pairs of $|\pm 1/2\rangle \leftrightarrow |\pm 3/2\rangle$ and $|\pm 3/2\rangle \leftrightarrow |\pm 5/2\rangle$ transitions the "satellite transitions" (STs). Here, we will designate these satellite pairs as ST(3/2) and ST(5/2), respectively. In a single crystal of LiAlO$_2$, one type of magnetically inequivalent ^{27}Al will therefore generate five resonance lines in the NMR spectrum. With four LiAlO$_2$ formula units per unit cell, a maximum of 20 resonance lines is expected. The four aluminum atoms in the unit cell occupy Wyckoff position 4a and are generated by rotations around 4-fold screw axes. Since the translatory component does not affect the NMR spectra, we can express the relation of the four ^{27}Al by successive rotations:

$$\underset{(x,x,0)}{\mathrm{Al}(1)} \xrightarrow{90^\circ} \underset{\left(\bar{x}+\frac{1}{2},x+\frac{1}{2},\frac{1}{4}\right)}{\mathrm{Al}(2)} \xrightarrow{90^\circ} \underset{\left(\bar{x},\bar{x},\frac{1}{2}\right)}{\mathrm{Al}(3)} \xrightarrow{90^\circ} \underset{\left(x+\frac{1}{2},\bar{x}+\frac{1}{2},\frac{3}{4}\right)}{\mathrm{Al}(4)}$$

Under each type of aluminum, the coordinates are listed, expressed in the coordinate system of the crystal lattice.

In order to properly evaluate the NMR spectra of single crystals, it is generally useful to clearly distinguish between three coordinate systems. Thus, the EFG tensor $\mathbf{V}$ of ^{27}Al in LiAlO$_2$ may be expressed in the laboratory (LAB) frame, where B_0 defines the z-axis, in the frame of the tetragonal crystal lattice (CRY), or in its own principal axis system (PAS), where it is diagonal:

$$\mathbf{V}^{LAB} \underset{\Omega_{CL}}{\overset{\Omega_{LC}}{\rightleftharpoons}} \mathbf{V}^{CRY} \underset{\Omega_{PC}}{\overset{\Omega_{CP}}{\rightleftharpoons}} \mathbf{V}^{PAS}$$

Here, the Ω_{XY} are the sets of Euler angles relating the X frame to the Y frame.[12] The positions of the CT and ST resonances of ^{27}Al in LiAlO$_2$ depend on the orientation of the crystal in the external magnetic field B_0. These positions change with the rotation of the crystal by the goniometer gear, in our case around an axis perpendicular to B_0. For each rotation angle φ, a different transformation Ω_{CL} applies. Three ^{27}Al NMR spectra resulting from such measurements are shown in Figure 2. The

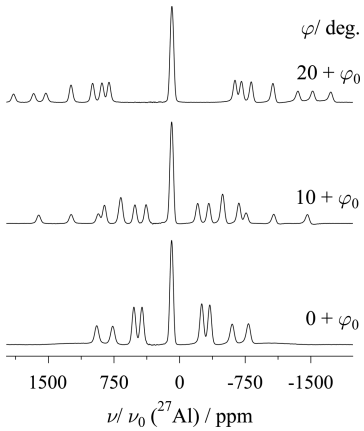

Figure 2. ^{27}Al NMR spectra of a single crystal of γ-LiAlO$_2$, rotated counterclockwise by the angle φ around a rotation axis perpendicular to the external magnetic field B_0. In the crystal frame, the rotation axis has a deviation of $\epsilon = 2.41°$ in the ab plane from the [110] direction. The zero point for the rotation, $\varphi = 0$, is defined by B_0 being parallel to the [001] direction, with the actual crystal orientation deviating by $\varphi_0 = 0.46°$ from it (see text for details).

splittings of the respective ST doublets, $\Delta\nu(\mathrm{ST}) = (\nu_+ - \nu_-)$, depend only on the quadrupolar interaction. Therefore, the EFG tensor of ^{27}Al can be derived from the orientation dependence of the $\Delta\nu(\mathrm{ST})$, which are plotted in Figure 3. The evolution of the splittings with the rotation angle φ follows the general expression[13]

$$\Delta\nu(\mathrm{ST}) = (\nu_+ - \nu_-) = A + B\cos 2\varphi + C\sin 2\varphi \tag{7}$$

The factors A, B, and C are combinations of the EFG tensor elements depending on the orientation of the PAS frame in the LAB frame. Since the NMR experiments are carried out in the LAB frame, it is customary to evaluate them in this frame using eq 7. However, for γ-LiAlO$_2$, it is advantageous to analyze the NMR spectra in the tetragonal crystal frame, since the high symmetry simplifies the tensors. With a small change in notation, we follow the procedure described for ^{7}Li NMR on lithium aluminate single crystals[1] and write the simplified EFG tensor for Al(1) as

DOI: 10.1021/acs.jpca.6b07286
J. Phys. Chem. A 2016, 120, 7839−7846

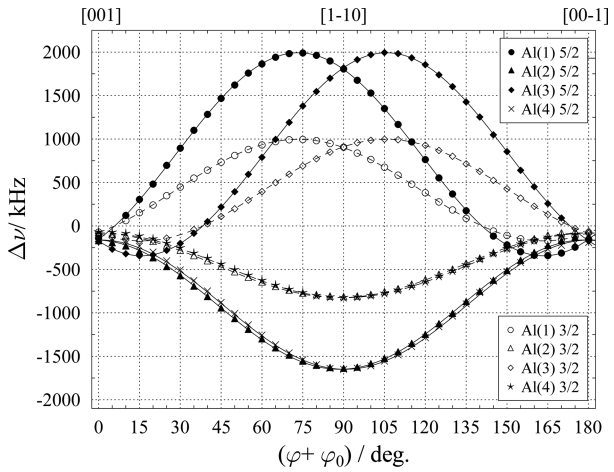

Figure 3. Plot of the splittings $\Delta\nu = (\nu_+ - \nu_-)$ for the ST(3/2) and ST(5/2) doublets of all four magnetically inequivalent ^{27}Al in the unit cell of the γ-$LiAlO_2$ single crystal. The experimental data points are plotted together with the lines representing the simultaneous (3 + 2) parameter fit (E, F, $G + \epsilon$, φ_0) of the EFG tensor. Above the plot, special orientations of the magnetic field in the crystal frame at $\varphi = 0°$, 90°, and 180° are indicated.

$$\mathbf{V}^{\mathrm{CRY}}_{\mathrm{Al}(1)} = \begin{pmatrix} V_{xx} & V_{xy} & V_{xz} \\ V_{yx} & V_{yy} & V_{yz} \\ V_{zx} & V_{zy} & V_{zz} \end{pmatrix} = \begin{pmatrix} E & F & G \\ F & E & -G \\ G & -G & -2E \end{pmatrix} \tag{8}$$

Here, we have made use of the facts that EFG tensors are in general symmetric and traceless, that is, $V_{ij} = V_{ji}$ and $V_{xx} + V_{yy} + V_{zz} = 0$. Furthermore, due to the tetragonal symmetry of the crystal structure and the 4-fold screw axes generating the positions of the symmetry-related aluminum atoms, we get $V_{xx} = V_{yy}$, and V_{xz} and V_{yz} differ only by their sign. In the crystal frame, the magnetic field B_0 will have a general orientation depending on the rotation angle φ, which may be described by the normal vector $\mathbf{b}(\varphi)$. The splittings for the satellite pairs of Al(1) observed for a specific orientation i can then be expressed as

$$\begin{aligned} \Delta\nu^i_{\mathrm{Al}(1)}(\varphi^i) &= \frac{3}{5f}\frac{eQ}{h}\cdot\mathbf{b}^{\mathrm{T}}(\varphi^i)\mathbf{V}^{\mathrm{CRY}}_{\mathrm{Al}(1)}\mathbf{b}(\varphi^i) \\ &= \frac{3}{5f}\frac{eQ}{\hbar}[E(b^i_x b^i_x + b^i_y b^i_y - 2b^i_z b^i_z) + F(2b^i_x b^i_y) \\ &\quad + G(2b^i_x b^i_z - 2b^i_y b^i_z)] \end{aligned} \tag{9}$$

The factor in the denominator is $f = 2$ for the ST(3/2) and $f = 1$ for the ST(5/2) transitions. Equations of this type can be used to fit the experimental data (see below) and thus determine the elements E, F, and G, which fully describe the EFG tensor of the ^{27}Al in the crystal frame.

The Chemical Shift (CS) Tensor. The positions of the centers of the satellite doublets (cST), as well as the position of the central transition (CT) depend on *both* the quadrupolar interaction (sometimes called quadrupolar-induced shift) and the chemical shift. The effect of the quadrupolar interaction on these positions in dependence on the rotation angle φ may be written as

$$\begin{aligned} \nu(\mathrm{cST,\ CT}) &= \frac{\nu_+ + \nu_-}{2} \\ &= A + B\cos 2\varphi + C\sin 2\varphi + B'\cos 4\varphi \\ &\quad + C'\sin 4\varphi \end{aligned} \tag{10}$$

If this contribution is subtracted from the experimental values, the remaining variation with the rotation angle is solely due to the chemical shift, and is again described by a relation of the type shown in eq 7. By convention, only the symmetric part of the chemical shift tensor is considered. Using the same symmetry arguments as for the EFG tensor above, the CS tensor for Al(1) in the crystal frame of γ-$LiAlO_2$ is given by

$$\boldsymbol{\delta}^{\mathrm{CRY}}_{\mathrm{Al}(1)} = \begin{pmatrix} \delta_{xx} & \delta_{xy} & \delta_{xz} \\ \delta_{yx} & \delta_{yy} & \delta_{yz} \\ \delta_{zx} & \delta_{zy} & \delta_{zz} \end{pmatrix} = \begin{pmatrix} P & Q & R \\ Q & P & -R \\ R & -R & S \end{pmatrix} \tag{11}$$

The weighted trace of $\boldsymbol{\delta}$ determines the isotropic chemical shift,

$$\delta_{\mathrm{iso}} = \frac{1}{3}\sum_i \delta_{ii} \tag{12}$$

Similar to the EFG tensor, an asymmetry parameter for the CS tensor may be defined:

$$\eta_{\mathrm{CS}} = \frac{\delta^{\mathrm{PAS}}_{yy} - \delta^{\mathrm{PAS}}_{xx}}{\Delta\delta} \tag{13}$$

Here, we order the tensor components according to the convention

$$|\delta_{zz} - \delta_{\mathrm{iso}}| \geq |\delta_{xx} - \delta_{\mathrm{iso}}| \geq |\delta_{yy} - \delta_{\mathrm{iso}}| \tag{14}$$

and have made use of the "reduced anisotropy", $\Delta\delta = \delta_{zz} - \delta_{\mathrm{iso}}$. The effect of the chemical shift on the positions of the satellite pair centers and the central transition for a specific orientation i of the magnetic field vector $\mathbf{b}(\varphi^i)$ can be expressed as

$$\begin{aligned} \nu^i_{\mathrm{Al}(1)}(\varphi^i) &= \mathbf{b}^{\mathrm{T}}(\varphi^i)\boldsymbol{\delta}^{\mathrm{CRY}}_{\mathrm{Al}(1)}\mathbf{b}(\varphi^i) \\ &= P(b^i_x b^i_x + b^i_y b^i_y) + Q(2b^i_x b^i_y) \\ &\quad + R(2b^i_x b^i_z - 2b^i_y b^i_z) + S(b^i_z b^i_z) \end{aligned} \tag{15}$$

The determination of the actual EFG and CS tensors for the ^{27}Al in lithium aluminate is described in the following.

3. RESULTS AND DISCUSSION

A melt-grown crystal of γ-$LiAlO_2$ with known morphology was used for the single-crystal NMR experiments. The crystal was mounted on a goniometer with the rotation axis perpendicular to the external magnetic field B_0. The crystal was glued on a support with its (001) face, with the [110] direction oriented parallel to the rotation axis. For the initial position of the crystal in the magnetic field, it was attempted to bring the [001] direction parallel to B_0. As detailed below, the resulting data indicate small misalignments for both rotation axis and initial orientation. Therefore, we will use the following expression to describe the magnetic field vector in the CRY frame for each rotation angle φ^i:

DOI: 10.1021/acs.jpca.6b07286
J. Phys. Chem. A 2016, 120, 7839−7846

$$\mathbf{b}(\varphi^i) = (\cos(45 + \epsilon)\sin(\varphi^i + \varphi_0) \quad \sin(45 + \epsilon)\sin(\varphi^i + \varphi_0) \quad \cos(\varphi^i + \varphi_0))^{\mathrm{T}} \tag{16}$$

Here, ϵ quantifies the deviation of the rotation axis from the [110] direction, which we assume to occur in the *ab* plane where the crystal is glued. The uncertainty of the initial position is taken into account by φ_0. Both parameters will be determined from fitting the experimental data.

Representative ^{27}Al NMR spectra are shown in Figure 2, which were obtained by rotating the crystal counterclockwise in steps of 5° using the goniometer gear. It can be seen that the central transition signals of the four independent ^{27}Al in the crystal structure are not resolved. The doublets of the ST(3/2) and ST(5/2) satellites can be clearly distinguished by their different intensities. All ^{27}Al resonance lines are comparatively broad (full width half-maximum, fwhm ≈ 5 kHz), which we attribute to the dipolar interaction between the aluminum (and to some extent lithium) atoms in the structure.[14]

Determination of the EFG Tensor. The experimentally determined quadrupole splittings of the ST(3/2) and ST(5/2) doublets are plotted over the rotation angle in Figure 3. The evolution of the splittings is mirrored at the direction where the magnetic field lies in the *ab* plane of the crystal frame, that is, along the [1$\bar{1}$0] direction. Furthermore, it can be seen that the experimental points for Al(2) and Al(4) are very close to each other. In fact, if the orientation of our rotation axis would be precisely along the [110] direction in the crystal frame, the splittings for Al(2) and Al(4) should be identical for each orientation. Their slightly diverging positions indicate a small misalignment of the rotation axis. Similarly, for the spectrum acquired for the nominal orientation φ = 0° in Figure 2, B_0 should be exactly parallel to the *c*-axis or [001]direction. For such orientation, all satellite transitions should be degenerate, since the *zz*-elements of all four ^{27}Al EFG tensors are identical. We do however observe a pairwise split of the ST(3/2) and ST(5/2) resonances, showing a small misalignment of the starting position.

To determine the components of the EFG tensor, the experimental splittings are fitted to eq 9 for Al(1), with the orientation of the magnetic field in the crystal frame given by eq 16. For a rotation around a general orientation (such as our axis), the three independent tensor components *E*, *F*, and *G* remaining in the tetragonal symmetry of γ-$LiAlO_2$ can in principle be determined from fitting a single satellite transition of Al(1). Therefore, a simultaneous fit for the four magnetically independent ^{27}Al in the unit cell produces an overdetermined system, which allows us to also derive values for the misalignment parameters ϵ and φ_0. To improve overall accuracy, both the ST(3/2) and ST(5/2) splittings have been included into the fit. For fitting the symmetry-related Al(2), Al(3), and Al(4), equations similar to eq 9 were used, which retain the same algebraic structure except for some sign changes. The data fit was performed with a purpose-written MatLab routine, giving ϵ = 2.41° and φ_0 = 0.46°. That is, if we express directions in polar angles in the CRY frame, the actual rotation axis is described by (90°, 47.41°) and the starting direction of $\mathbf{b}(\varphi_0)$ by (0.46°, 315°) instead of the (90°, 45°) and (0°, 0°) we were initially aiming for. The plot in Figure 3 shows that the harmonics generated from the fitted tensor nicely approximate the experimental data. It should be noted, however, that the tensor actually fitted from the experimental splitting is not the EFG directly but rather the quadrupole coupling tensor, $(eQ/\hbar)\mathbf{V}$, which in its diagonalized form has $\chi = C_Q$ as its *zz* component. From the residuals of the fit, the error of tensor components can be determined,[15] yielding in our case about ±2.5 kHz. To account for other subtle errors (e.g., inaccuracies of the goniometer gear), this number can be doubled to arrive at an upper error limit of ±5 kHz, which is amply dimensioned and probably somewhat lower than that. The quadrupole coupling constant (eq 4) of ^{27}Al in γ-$LiAlO_2$ derived from our NMR experiments is therefore $\chi = C_Q$ = 3.330 ± 0.005 MHz. This value of χ is about 29 times larger than the corresponding value for ^{7}Li (115 kHz[1]) in the γ-$LiAlO_2$ crystal structure. The large difference is caused both by the larger *Q* value of ^{27}Al (about 3.7 times larger) and the $V_{zz}^{PAS} = eq$ value at the aluminum site, which is about 7.9 times larger than that of ^{7}Li. The asymmetry parameter (eq 5), reflecting the deviation of the electronic surroundings from cylindrical symmetry, is η_Q = 0.656 ± 0.002, which is very close to that of ^{7}Li, 0.690.[1] Previously reported ^{27}Al quadrupolar parameters for γ-$LiAlO_2$, from static and MAS spectra of a polycrystalline sample, are χ = 3.2 MHz and η_Q = 0.70.[3] To obtain the EFG tensor, the quadrupole coupling tensor needs to be divided by the nuclear quadrupole moment *Q* (and fundamental constants). Here, the reported uncertainty of about 0.7%, *Q* = (146.6 ± 1.0) mb,[11] becomes the dominant source of error. Taking into account both errors, and propagation by division, the EFG tensor components for the Al(1) site can be given with the following error:

$$E = V_{xx} = V_{yy} = -\frac{1}{2}V_{zz} = (0.38 \pm 0.05) \times 10^{20}\ \mathrm{V/m^2}$$

$$F = V_{xy} = V_{yx} = -(8.16 \pm 0.05) \times 10^{20}\ /\mathrm{m^2}$$

$$G = V_{xz} = -V_{yz} = (2.08 \pm 0.05) \times 10^{20}\mathrm{V/m^2}$$

Diagonalization of the full EFG tensor in the CRY frame (eq 8) then gives the eigenvalues and eigenvectors listed in Table 1.

Table 1. EFG Tensor[a] of ^{27}Al in γ-$LiAlO_2$

	Single-Crystal NMR[b]	DFT (CASTEP)
V_{xx}^{PAS}	−1.61 × 10^{20} V/m^2	−1.37 × 10^{20} V/m^2
V_{yy}^{PAS}	−7.78 × 10^{20} V/m^2	−8.11 × 10^{20} V/m^2
V_{zz}^{PAS}	+9.40 × 10^{20} V/m^2	+9.49 × 10^{20} V/m^2
$\vec{e}_{xx}$	(−0.197 0.197 0.960)	(−0.188 0.188 0.964)
$\vec{e}_{yy}$	(0.707 0.707 0.000)	(0.707 0.707 0.000)
$\vec{e}_{zz}$	(−0.679 0.679 −0.278)	(−0.681 0.681 −0.266)
$\chi = C_Q$	3.330 ± 0.005 MHz	3.363 MHz
η_Q	0.656 ± 0.002	0.710

[a]Eigenvectors (in the crystal frame) and eigenvalues, as determined by single-crystal NMR and DFT calculations. [b]All experimentally determined EFG components have an estimated error of ±0.05 × 10^{20} V/m^2, see text for details.

Since the early 2000s, it has become increasingly common within the solid-state NMR community to augment experimental results by comparing them to predictions derived from calculations using density functional theory (DFT). Numerous studies have demonstrated that DFT methods employing periodic plane waves are capable of calculating NMR interaction parameters from structural data to a sufficiently high degree to be meaningful.[16] In order to check how DFT predictions match with our comparatively precise single-crystal results, we have performed such calculations for γ-$LiAlO_2$, using

DOI: 10.1021/acs.jpca.6b07286
J. Phys. Chem. A 2016, 120, 7839−7846

the CASTEP code (see section 5 for details). It is usually necessary to energy-optimize the atomic coordinates stemming from diffraction studies by the DFT algorithm, since it is well documented in the literature that structure optimization is necessary to achieve good agreement between experiments and calculations.[17−19] We performed this energy optimization using the coordinates from X-ray diffraction[4] as a starting point (using the coordinates of neutron diffraction[5] gave essentially identical results). As may be seen from Table 1, both the eigenvalues and eigenvectors of the EFG tensor determined by the DFT calculations are in good quantitative agreement with the experiment.

Determination of the CS Tensor. The chemical shift (CS) tensor affects the absolute positioning of the ^{27}Al multiplets comprised of central transition (CT) and satellite transitions (ST's). However, as stated above, these positions depend on the chemical shift and the shift induced by the quadrupole interaction. After subtracting the effect of the quadrupolar coupling, the chemical shift tensor may be determined from the remaining orientation dependence of the resonances. In most instances in the literature, this procedure was carried out using the CT signal.[20−22] In γ-$LiAlO_2$, the CT contributions of all four aluminum atoms overlap over the entire rotation pattern. In such a case, the variation of the centers of STs may be traced instead, as was done, for example, by Hansen et al.[23] In Figure 4, the centers of

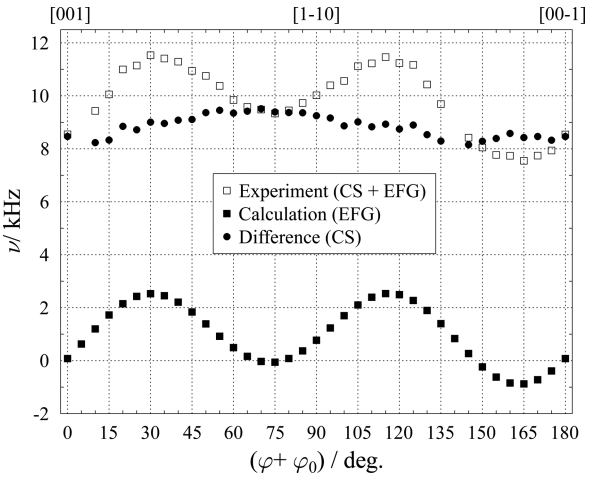

Figure 4. Plot of the satellite centers, $\nu(\mathrm{cST}) = (\nu_+ + \nu_-)/2$, for the ST(5/2) doublets of Al(1). The experimental data clearly show the presence of higher order harmonics according to eq 10. After subtracting the contribution of the quadrupolar interaction (calculated using the experimentally determined EFG tensor), only harmonics according to eq 7 remain, which reflect the orientation dependence of the chemical shift tensor.

the individual ST(5/2) resonances are plotted for Al(1). The data points clearly show the presence of higher order harmonics according to eq 10. Using the EFG tensor determined above, the shift due to the quadrupole interaction can be calculated for each crystal orientation. To do this, we transformed each orientation in the CRY frame into the PAS frame of the EFG tensor. Then, the matrix representation of the quadrupolar Hamiltonian (eq 3) was diagonalized to obtain the resonance frequencies under quadrupole interaction only. It can be seen in Figure 4 that after subtracting the quadrupolar contribution from the experimental points, only harmonics according to eq 7 remain, which reflect the orientation dependence of the chemical shift tensor.

We note that in contrast to the traceless EFG tensor, the four components of the CS tensor may not be determined from the data of a single aluminum atom. The set of linearly independent data can be expanded by either recording additional rotation patterns around different axes or by including the information supplied by the symmetry-related atoms in the crystal structure. The latter approach is sometimes referred to as "single rotation method".[24,25] (In some special cases, the internal crystal symmetry may even be exploited to determine the orientation of the rotation axis.[26]) To utilize the data of the four magnetically inequivalent but symmetry-related ^{27}Al in γ-$LiAlO_2$, the quadrupolar correction was performed for all of them, with the resulting data points plotted in Figure 5.

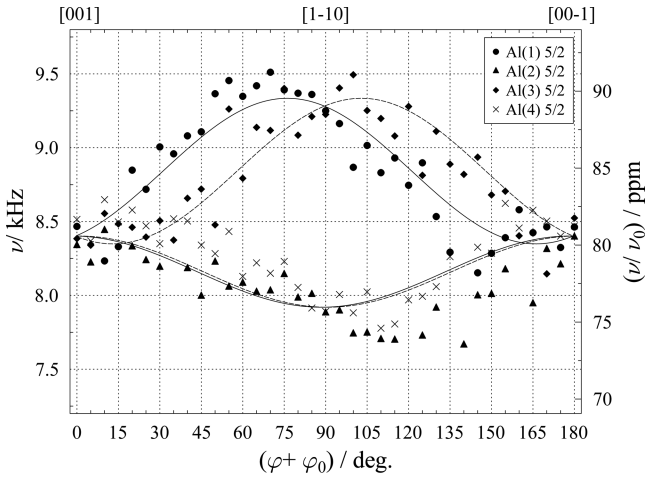

Figure 5. Plot of the ST(5/2) doublet centers corrected for the quadrupolar contribution (see Figure 4) for all four magnetically inequivalent ^{27}Al in the unit cell of γ-$LiAlO_2$. The experimental data points are plotted together with the lines representing the simultaneous four-parameter fit (P, Q, R, S) of the chemical shift (CS) tensor, with the additional parameters $\epsilon = 2.41°$ and $\varphi_0 = 0.46°$ fixed.

(Missing points indicate overlap of resonances, which made a precise determination of the line position difficult.) When plotted at the scale used in Figure 5, the data exhibit quite some scatter. It has to be kept in mind however that for tracing the anisotropy of the ^{27}Al chemical shift in γ-$LiAlO_2$, we are attempting to extract variations of the order of ∼1 kHz from resonance lines with fwhm ≈ 5 kHz. This scatter was even more pronounced for the ST(3/2) data, so for the CS fit, only the ST(5/2) data were used for each aluminum atom. The full CS tensor was then extracted from the data in Figure 5 by a simultaneous fit according to eq 15 (and their symmetry-related counterparts), with the orientation of the magnetic field in the crystal frame again given by eq 16. For this fit, the actual orientation of the rotation axis and the starting direction were kept fixed at the values derived from the EFG tensor fit as described above. The components of the chemical shift tensor at the Al(1) site determined by the fit are

DOI: 10.1021/acs.jpca.6b07286
J. Phys. Chem. A 2016, 120, 7839−7846

$$P = \delta_{xx} = \delta_{yy} = (82.4 \pm 0.1)\ \text{ppm}$$

$$Q = \delta_{xy} = \delta_{yx} = (-6.5 \pm 0.1)\ \text{ppm}$$

$$R = \delta_{xz} = -\delta_{yz} = (1.5 \pm 0.1)\ \text{ppm}$$

$$S = \delta_{zz} = (80.6 \pm 0.1)\ \text{ppm}$$

Here, the uncertainties of ±0.1 ppm reflect only the error derived from the fit residuals. The overall error (including the quadrupolar correction) is estimated to be of the order of ±0.25 ppm. In spite of the considerable data scatter, the harmonics resulting from the fitted CS tensor reproduce the experimental results rather well. It may also be seen from Figure 5 that the variation caused by the CS is better defined for Al(1) and Al(2) than for Al(3) and Al(4). Fitting only Al(1) and Al(2) gave results that were practically identical to the fit that included all four ^{27}Al in the unit cell. The diagonalization of the full CS tensor in the crystal frame (eq 11) gives the eigenvalues and eigenvectors listed in Table 2. We note that the

Table 2. Chemical shift (CS) Tensor[a] of ^{27}Al in γ-$LiAlO_2$

	Single-Crystal NMR[b]	DFT (CASTEP)[c]	MAS NMR
δ_{xx}^{PAS}	75.9 ppm	75.6 ppm	
δ_{yy}^{PAS}	80.0 ppm	75.9 ppm	
δ_{zz}^{PAS}	89.5 ppm	89.7 ppm	
$\vec{d}_{xx}$	(0.707 0.707 0.000)	(0.161 −0.161 −0.974)	
$\vec{d}_{yy}$	(0.163 −0.163 −0.972)	(−0.707 −0.707 0.000)	
$\vec{d}_{zz}$	(−0.688 0.688 −0.231)	(−0.688 0.688 0.228)	
δ_{iso}	81.8 ± 0.25 ppm	80.4 ppm	81.0 ppm
$\Delta\delta$	7.7 ppm	9.3 ppm	11.0 ppm
η_{CS}	0.532 ± 0.004	0.03	0.40

[a]Eigenvectors (in the crystal frame) and eigenvalues, as determined by single-crystal NMR, DFT calculations, and MAS NMR. [b]All experimentally determined CS components have an estimated error of ±0.25 ppm; see text for details. [c]The shieldings σ computed by CASTEP have been converted to chemical shifts δ using the empirical relation δ = 549.8 ppm − 0.9927σ; see text for details.

PAS frames spanned by the eigenvectors of the CS and EFG tensors, as determined from our single-crystal data, are practically colinear, with deviations being <3°. This gives further confidence in the quality of the data fit, since such colinearity can hardly arise by coincidence. Also, the asymmetry parameter of the CS tensor, η_{CS} = 0.532 ± 0.004, is close to that of the EFG tensor, indicating a biaxiality in the electronic surroundings of ^{27}Al for both tensors.

The ^{27}Al isotropic shift for γ-$LiAlO_2$ derived from our fitted tensor is 81.8 ppm, which is in the range expected for aluminum tetrahedrally coordinated by oxygen.[27,28] Information about the chemical shift may also be obtained from magic-angle spinning (MAS) NMR experiments. An ^{27}Al NMR spectrum from a polycrystalline γ-$LiAlO_2$ sample acquired at 10 kHz spinning speed and a magnetic field of B_0 = 21.1 T is shown in Figure 6. This spectrum was fitted using the SOLA module of the TOPSPIN spectrometer software. For the fit, the effects of the quadrupolar interaction on the spectrum were taken into account by using the EFG parameters determined from our single-crystal analysis. The isotropic shift derived from the MAS fit is 81.0 ppm and thus very close to the value from single-crystal NMR. Other CS tensor parameters (see Table 2) agree less well, but we note that a multiparameter fit of such a large spinning sideband manifold is fraught with difficulties.

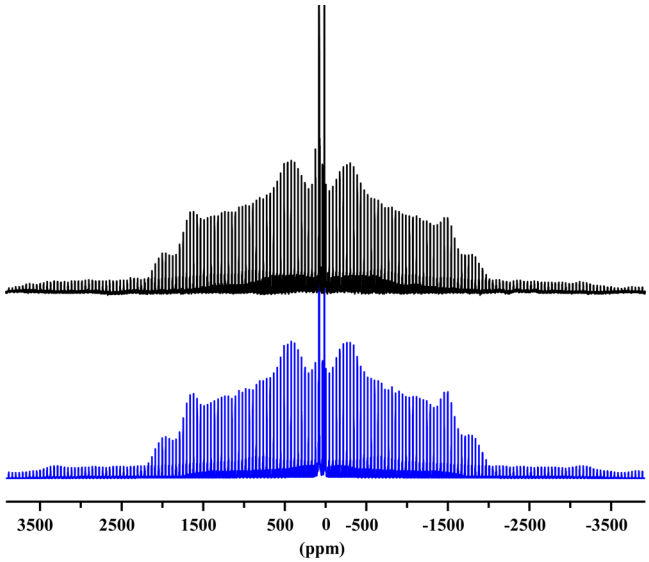

Figure 6. ^{27}Al NMR MAS spectra of a polycrystalline sample of γ-$LiAlO_2$. (top) Experimental spectrum, acquired with ν_{MAS} = 10 kHz and B_0 = 21.1 T. (bottom) Simulated spectrum using fixed quadrupolar interaction parameters (from single-crystal data) to extract information about the chemical shift, with the results listed in Table 2. With much lower intensity, the presence of a second spinning sideband manifold is visible. From its isotropic shift of 15.3 ppm, we attribute this to α-$LiAlO_2$,[3] an impurity phase in the purchased sample.

Already in 1983, Müller et al.[3] determined the ^{27}Al isotropic shift of γ-$LiAlO_2$ from static and MAS spectra of a polycrystalline sample to be 82 ppm, which is remarkably close to our value.

We can also correlate our experimentally determined CS tensor to the DFT calculations carried out with the CASTEP program. To convert the magnetic shielding constants produced by CASTEP to experimental chemical shifts, a calibration plot of previously measured and calculated compounds with ^{27}Al in oxygen coordination was employed (unpublished results). The empirical linear relation resulting from this plot is given in the caption of Table 2. Looking at the eigenvalues and eigenvectors of the CS tensor from the CASTEP calculations (see Table 2), it may be seen that the direction of the eigenvectors agree very well with the experiment. Here, the comparison is not entirely straightforward, since assigning the tensor eigenvalues by convention of eq 14 necessitates a reordering. This reordering is a result of the CASTEP eigenvalues, which give a CS tensor that is almost uniaxial. This is in stark contrast to both the EFG and CS tensor derived from the single-crystal NMR data. For reasons outlined above, we believe the single-crystal CS tensor to be accurate within the given error limits. Therefore, the discrepancy between NMR and DFT results rather points to shortcomings of the computational method. One may particularly note that due to the rather small CSA, small miscalculations in the components δ_{xx}^{PAS} and δ_{yy}^{PAS} will result in large variation of the calculated η_{CS}. The problem that the smaller tensor components are determined imprecisely by calculations, while the principal component (EFG) respectively isotropic shift (CS) is very close to the experimental value indeed occurs quite frequently.[16−19]

DOI: 10.1021/acs.jpca.6b07286
J. Phys. Chem. A 2016, 120, 7839−7846

4. CONCLUSIONS

Utilizing the high precision inherent in single-crystal NMR experiments, we have determined the full tensors for both the electrical field gradient (EFG) and the chemical shift (CS) for ^{27}Al in γ-$LiAlO_2$. Because of the high symmetry of the tetragonal crystal, it proved convenient to perform the tensor determination in the crystal frame. A simultaneous fit for all four aluminum atoms in the unit cell gave the full EFG tensor, yielding eigenvalues and eigenvectors after diagonalization. Thus, the quadrupolar coupling constant of ^{27}Al in γ-$LiAlO_2$ is $\chi = C_Q = 3.330 \pm 0.005$ MHz, with asymmetry $\eta_Q = 0.656 \pm 0.002$. The experimentally determined quadrupolar splittings were sufficiently sensitive to quantify small deviations of both rotation axis direction and starting direction by the data fitting routine. To extract the CS tensor, the evolution of the ST(5/2) satellite centers over the crystal rotation was tracked, and the contribution of the quadrupolar shift was subtracted according to the previously determined EFG tensor. Again, a simultaneous fit for all four ^{27}Al gave the full CS tensor in the crystal frame, yielding eigenvalues and eigenvectors after diagonalization. The resulting isotropic chemical shift is $\delta_{iso} = 81.8 \pm 0.25$ ppm, in good agreement with our MAS NMR results and a previously reported value.[3] The asymmetry parameter of the CS tensor, $\eta_{CS} = 0.532 \pm 0.004$, is close to that of the EFG tensor. From both experiments and DFT calculations, we find the eigenvectors of the EFG and CS tensors to be practically colinear, with deviations being <3°. Interestingly, for one of the lesser tensor components (V_{yy}^{PAS} and δ_{xx}^{PAS}), the corresponding eigenvector is aligned exactly along the diagonal of the *ab*-plane in the crystal frame. This is a consequence of the symmetry enforced by 2-fold rotation axes in the tetragonal unit cell, on which the ^{27}Al atoms (at Wyckoff positions 4*a*) are located. The same effect was also found for the ^{7}Li atoms in γ-$LiAlO_2$,[1] which are similarly positioned at 4*a*. As it happens, this diagonal (or [110] direction) is also the connecting line between lithium and aluminum atoms in the crystal structure, as may be seen from Figure 7. The screw axes in space group $P4_12_12$, which are oriented parallel to the crystallographic *c*-axis, do not impose additional symmetry constraints on either ^{7}Li or ^{27}Al. Therefore, the remaining tensor eigenvectors do not align along special directions in the crystal frame but are free to orient according to the electronic environment generated chiefly by the surrounding oxygen atoms. Thus, as one might expect, the local electronic structure in γ-$LiAlO_2$, as represented by EFG and CS tensor determined from single-crystal NMR experiments, reflects the features of the crystal structure.

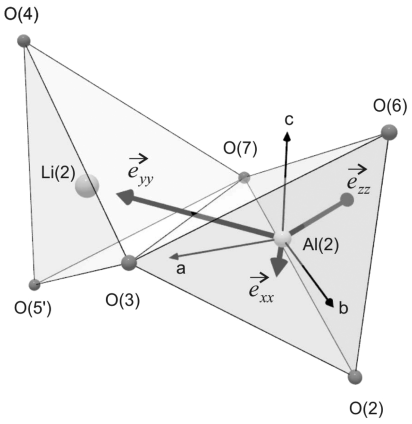

Figure 7. Elementary unit of the γ-$LiAlO_2$ crystal structure, consisting of a pair of LiO_4 and AlO_4 tetrahedra connected via a common edge. The bold arrows show the principal axes of the ^{27}Al EFG tensor, with their length scaled to the corresponding eigenvalues. The thin arrows show the principal axes of the tetragonal crystal frame. The equivalent representation for ^{7}Li may be found in ref 1.

5. EXPERIMENTAL DETAILS

5.1. Lithium Aluminate. Single crystals of γ-$LiAlO_2$ were grown using the Czochralski technique with radio frequency induction heating, as described in detail in ref 1. The polycrystalline sample of γ-$LiAlO_2$ was purchased from Sigma-Aldrich and used without further purification.

5.2. Solid-State ^{27}Al NMR. Single-crystal ^{27}Al NMR spectra were acquired on a Bruker Avance-III 400 spectrometer, at a Larmor frequency of $\nu_0(^{27}Al) = 104.263$ MHz, using a goniometer probe with a solenoid coil, built by NMR Service GmbH (Erfurt, Germany). ^{27}Al MAS spectra were acquired on a Bruker Avance-II 900 spectrometer, at a Larmor frequency of $\nu_0(^{27}Al) = 226.657$ MHz, with the polycrystalline sample in a 4 mm rotor spinning at 10 kHz. Recycle delays were of the order of 10 s. All spectra were referenced to a dilute $Al(NO_3)_3$ solution at 0 ppm.

5.3. DFT Calculations. All calculations were performed with the CASTEP density functional theory (DFT) code[29] using the GIPAW algorithm.[30] The version used in this work is integrated within the Accelrys Materials Studios 4.4 suite. The computations use the generalized gradient approximation (GCA) and Perdew–Burke–Ernzerhof (PBE) functional,[31] with the core–valence interactions described by ultrasoft pseudopotentials.[30] Integrations over the Brillouin zone were done using a Monkhorst–Pack grid[32] with *k* point spacings generally being less than 0.04 $Å^{-1}$. The cutoff energy used was in the range of 550–610 eV. The convergence of the calculated NMR parameters was tested for both the size of a Monkhorst–Pack *k*-grid and a basis set cutoff energy. Geometry optimization calculations were performed using the Broyden–Fletcher–Goldfarb–Shanno (BFGS) algorithm,[33] with the same functional, *k*-grid spacings, and cutoff energies as in the single-point energy calculations. Convergence tolerance parameters for geometry optimization were as follows: maximum energy 2.0×10^{-5} eV/atom, maximum force 0.05 eV/Å, maximum stress 0.1 GPa, and maximum displacement 0.002 Å. Crystallographic data used in the calculations were taken from the literature.[4,5]

AUTHOR INFORMATION

Corresponding Authors

*Tel. +49-89-2180-77433. E-mail: thomas.braeuniger@cup.lmu.de.

*Tel. +49-721-608-28508. E-mail: sylvio.indris@kit.edu.

Notes

The authors declare no competing financial interest.

ACKNOWLEDGMENTS

The authors are grateful to J. Haase (University of Leipzig) for valuable discussions concerning the diagonalization of quadrupolar Hamiltonians, to C. Hoch (University of Munich, LMU) for helpful advice in crystallographic matters, and to V. Terskikh (University of Ottawa, Canada) for stimulating discussions and access to computational resources. Also, we thank T. Bredow (University of Bonn) for performing some

DOI: 10.1021/acs.jpca.6b07286
J. Phys. Chem. A 2016, 120, 7839–7846

initial DFT calculations for ^{27}Al in γ-$LiAlO_2$ and R. Uecker (IKZ Berlin) for supplying the single crystal. Access to the 900 MHz NMR spectrometer was provided by the National Ultrahigh Field NMR Facility for Solids (Ottawa, Canada), a national research facility funded by the Canada Foundation for Innovation, the Ontario Innovation Trust, Recherche Québec, and Bruker BioSpin and managed by the University of Ottawa (http://www.nmr900.ca).

REFERENCES

(1) Indris, S.; Heitjans, P.; Uecker, R.; Bredow, T. Local electronic structure in a $LiAlO_2$ single crystal studied with ^{7}Li NMR spectroscopy and comparison with quantum chemical calculations. *Phys. Rev. B: Condens. Matter Mater. Phys.* **2006**, *74*, 245120.

(2) Indris, S.; Heitjans, P.; Uecker, R.; Roling, B. Li Ion Dynamics in a $LiAlO_2$ Single Crystal Studied by ^{7}Li NMR Spectroscopy and Conductivity Measurements. *J. Phys. Chem. C* **2012**, *116*, 14243−14247.

(3) Müller, D.; Gessner, W.; Scheler, G. Chemical Shift and Quadrupole Coupling of the ^{27}Al NMR Spectra of $LiAlO_2$ Polymorphs. *Polyhedron* **1983**, *2*, 1195−1198.

(4) Marezio, M. The Crystal Structure and Anomalous Dispersion of γ-$LiAlO_2$. *Acta Crystallogr.* **1965**, *19*, 396−400.

(5) Wiedemann, D.; Indris, S.; Meven, M.; Pedersen, B.; Boysen, H.; Uecker, R.; Heitjans, P.; Lerch, M. Single-crystal neutron diffraction on γ-$LiAlO_2$: structure determination and estimation of lithium diffusion pathway. *Z. Kristallogr. - Cryst. Mater.* **2016**, *231*, 189−193.

(6) Cao, H.; Xia, B.; Zhang, Y.; Xu, N. $LiAlO_2$-coated $LiCoO_2$ as cathode material for lithium ion batteries. *Solid State Ionics* **2005**, *176*, 911−914.

(7) Lakshman Dissanayake, M. A. K. Nano-Composite Solid Polymer Electrolytes for Solid State Ionic Devices. *Ionics* **2004**, *10*, 221−225.

(8) Cohen, M. H.; Reif, F. Quadrupole Effects in Nuclear Magnetic Resonance Studies of Solids. In *Solid State Physics: Advances in Research and Applications* Seitz, F., Turnbull, D., Eds.; Academic Press: New York, 1957; Vol. *5*, pp 327−438.

(9) Jerschow, A. From nuclear structure to the quadrupolar NMR interaction and high-resolution spectroscopy. *Prog. Nucl. Magn. Reson. Spectrosc.* **2005**, *46*, 63−78.

(10) Freude, D.; Haase, J. www.quad-nmr.de.

(11) Pyykkö, P. Year-2008 nuclear quadrupole moments. *Mol. Phys.* **2008**, *106*, 1965−1974.

(12) Millot, Y.; Man, P. P. Active and passive rotations with Euler angles in NMR. *Concepts Magn. Reson., Part A* **2012**, *40A*, 215−252.

(13) Volkoff, G. M.; Petch, H. E.; Smellie, D. W. L. Nuclear electric quadrupole interactions in single crystals. *Can. J. Phys.* **1952**, *30*, 270−289.

(14) Silver, A. H.; Kushida, T.; Lambe, J. Nuclear magnetic dipole coupling in Al_2O_3. *Phys. Rev.* **1962**, *125*, 1147−1149.

(15) Vosegaard, T.; Hald, E.; Langer, V.; Skov, H. J.; Daugaard, P.; Bildsøe, H.; Jakobsen, H. J. Improved hardware and software for single-crystal NMR spectroscopy. *J. Magn. Reson.* **1998**, *135*, 126−132.

(16) Charpentier, T. The PAW/GIPAW approach for computing NMR parameters: A new dimension added to NMR study of solids. *Solid State Nucl. Magn. Reson.* **2011**, *40*, 1−20.

(17) Body, M.; Silly, G.; Legein, C.; Buzare, J.-Y.; Calvayrac, F.; Blaha, P. ^{27}Al NMR experiments and quadrupolar parameter ab initio calculations: Crystallographic structure refinement of β-Ba_3AlF_9. *Chem. Phys. Lett.* **2006**, *424*, 321−326.

(18) Cuny, J.; Messaoudi, S.; Alonzo, V.; Furet, E.; Halet, J.-F.; Le Fur, E.; Ashbrook, S. E.; Pickard, C. J.; Gautier, R.; Le Pollès, L. DFT calculations of quadrupolar solid-state NMR properties: Some examples in solid-state inorganic chemistry. *J. Comput. Chem.* **2008**, *29*, 2279−2287.

(19) Chandran, C. V.; Cuny, J.; Gautier, R.; Le Pollès, L.; Pickard, C. J.; Bräuniger, T. Improving sensitivity and resolution of MQMAS spectra: A ^{45}Sc-NMR case study of scandium sulphate pentahydrate. *J. Magn. Reson.* **2010**, *203*, 226−235.

(20) Vosegaard, T.; Jakobsen, H. J. ^{27}Al chemical shielding anisotropy. *J. Magn. Reson.* **1997**, *128*, 135−137.

(21) Vosegaard, T.; Byriel, I. P.; Pawlak, D. A.; Wozniak, K.; Jakobsen, H. J. Crystal structure studies on the garnet $Y_3Al_5O_{12}$ by ^{27}Al Single-Crystal NMR Spectroscopy. *J. Am. Chem. Soc.* **1998**, *120*, 7900−7904.

(22) Bryant, P. L.; Harwell, C. R.; Wu, K.; Fronczek, F. R.; Hall, R. W.; Butler, L. G. Single-crystal ^{27}Al NMR of andalusite and calculated electric field gradients: The first complete NMR assignment for a 5-coordinated aluminum site. *J. Phys. Chem. A* **1999**, *103*, 5246−5252.

(23) Hansen, M. R.; Vosegaard, T.; Jakobsen, H. J.; Skibsted, J. ^{11}B chemical shielding anisotropies in borates from ^{11}B MAS, MQMAS, and single-crystal NMR spectroscopy. *J. Phys. Chem. A* **2004**, *108*, 586−594.

(24) Weil, J. A. Use of symmetry-related crystal sites for measuring tensor properties in magnetic resonance. *J. Magn. Reson.* **1973**, *10*, 391−393.

(25) Tesche, B.; Zimmermann, H.; Poupko, R.; Haeberlen, U. The single-rotation method of determining quadrupole coupling tensors in monoclinic crystals. Error analysis and application to bullvalene. *J. Magn. Reson., Ser. A* **1993**, *104*, 68−77.

(26) Kye, Y.-S.; Zhao, X.; Harbison, G. S. Orientation of single crystals using linear approximations to NMR transits. *J. Magn. Reson.* **2005**, *174*, 54−59.

(27) Bräuniger, T.; Jansen, M. Solid-state NMR spectroscopy of quadrupolar nuclei in inorganic chemistry. *Z. Anorg. Allg. Chem.* **2013**, *639*, 857−879.

(28) Haouas, M.; Taulelle, F.; Martineau, C. Recent advances in application of ^{27}Al NMR spectroscopy to materials science. *Prog. Nucl. Magn. Reson. Spectrosc.* **2016**, *94*−*95*, 11−36.

(29) Segall, M. D.; Lindan, P. J. D.; Probert, M. J.; Pickard, C. J.; Hasnip, P. J.; Clark, S. J.; Payne, M. C. First-principles simulations: ideas, illustrations and the CASTEP code. *J. Phys.: Condens. Matter* **2002**, *14*, 2717−2744.

(30) Yates, J. R.; Pickard, C. J.; Mauri, F. Calculation of NMR chemical shifts for extended systems using ultrasoft pseudopotentials. *Phys. Rev. B: Condens. Matter Mater. Phys.* **2007**, *76*, 024401.

(31) Perdew, J. P.; Burke, K.; Ernzerhof, M. Generalized gradient approximation made simple. *Phys. Rev. Lett.* **1996**, *77*, 3865−3868.

(32) Monkhorst, H. J.; Pack, J. D. Special points for Brillouin-zone integrations. *Phys. Rev. B* **1976**, *13*, 5188−5192.

(33) Pfrommer, B. G.; Côté, M.; Louie, S. G.; Cohen, M. L. Relaxation of crystals with the quasi-Newton method. *J. Comput. Phys.* **1997**, *131*, 233−240.

DOI: 10.1021/acs.jpca.6b07286
J. Phys. Chem. A 2016, 120, 7839−7846